

COPYRIGHT WARNING

This paper is protected by copyright. You are advised to print or download **ONE COPY** of this paper for your own private reference, study and research purposes. You are prohibited having acts infringing upon copyright as stipulated in Laws and Regulations of Intellectual Property, including, but not limited to, appropriating, impersonating, publishing, distributing, modifying, altering, mutilating, distorting, reproducing, duplicating, displaying, communicating, disseminating, making derivative work, commercializing and converting to other forms the paper and/or any part of the paper. The acts could be done in actual life and/or via communication networks and by digital means without permission of copyright holders.

The users shall acknowledge and strictly respect to the copyright. The recitation must be reasonable and properly. If the users do not agree to all of these terms, do not use this paper. The users shall be responsible for legal issues if they make any copyright infringements. Failure to comply with this warning may expose you to:

- Disciplinary action by the Vietnamese-German University.
- Legal action for copyright infringement.
- Heavy legal penalties and consequences shall be applied by the competent authorities.

The Vietnamese-German University and the authors reserve all their intellectual property rights.



bachelor thesis

MODELING OF THE ADSORPTION KINETICS OF WATER VAPOR ON BIOMASS CHARs



Vietnamese-German University

Anh Duc Truong

November 2023

Modeling of the adsorption kinetics of water vapor on biomass chars



THERMODYNAMIK

VGU

Vietnamese-German University



THERMODYNAMIK

Bachelor Thesis

MODELING THE ADSORPTION KINETICS OF WATER VAPOR ON BIOMASS CHARs

Name: Truong Duc Anh
Matr. -No.: 1080020266108
Course of study: Mechanical Engineering



1. Reviewer: Prof. Dr.-Ing. Roland Span
2. Expert: Dr.-Ing. Monika Thol
Supervision: M. Sc. Tim Eisenbach

October 31, 2023

bachelor thesis of

Mr. Anh Duc Truong, Matr.-Nr.: 1080020266108

MODELING OF THE ADSORPTION KINETICS OF WATER VAPOR ON BIOMASS

CHARS (MODELLIERUNG DER ADSORPTIONSKINETIKEN VON WASSERDAMPF AUF BIOMASSE-KOKSEN)

In the course of efforts to reduce emissions of climate-damaging gases in the energy sector, oxyfuel processes can make a significant contribution. When solid fuels are converted in an oxyfuel atmosphere, which consists mainly of O₂, recirculated CO₂ and H₂O, the resulting CO₂ can be captured and stored much more easily using Carbon Capture, Utilization and Storage (CCUS) technologies. The novel physical properties of the combustion process in an oxyfuel atmosphere are becoming the focus of research. Important sub-processes in the combustion of solids are diffusion and sorption of the relevant gases in the pores or on the surfaces of the fuels. Compared to the gas adsorption of CO₂ and O₂, the adsorption of water vapor has a significantly different characteristic, which requires a fundamental revision of existing modeling approaches.

Aufgabe:

In the course of this thesis, an existing data basis of adsorption kinetics of water vapor for two investigated biomass chars should be used for the development of a novel adsorption kinetic model, which can further be used to predict the adsorptive behavior of water vapor beyond the experimental boundaries. In the first part of this thesis the experimental data basis should be adequately presented and set into the context of the dependency of water vapor adsorption on the porous structure and the quantity of oxygen functional groups of the investigated biomass chars. By working out the comprehensive dependencies of water vapor adsorption on pressure and temperature an appropriate model approach needs to be chosen and tested for the specific application and data basis. Another claim for this thesis is an extended parameter discussion and the proper presentation of the modeling results. Furthermore, a brief discussion of the results should be presented with respect to the capabilities of the novel modeling approach and the extrapolation behavior.

Please discuss details of the work to be carried out with your supervisor, Mr. Tim Eisenbach, M.Sc.

Prof. Dr.-Ing. R. Span

15. August 2023

Explanation

I, Truong Duc Anh , hereby declare that I have completed this work independently, apart from the contributions of the issuing professor and the supervisor. It was created without the unauthorized intervention of third parties. All tools used to create this work are documented in the bibliography. Everything that has been taken over from other works unchanged or with modifications is identified.

Bochum, October 2023



A handwritten signature in black ink, which appears to be 'Anh', is written above a solid horizontal line. The signature is fluid and cursive.

Truong Duc Anh

Table of contents

Frequently used symbols	2
1 Introduction.....	4
2 Adsorption kinetic modeling in char conversion	5
2.1 Current consideration of pore diffusion in char conversion modeling.....	5
2.2 A Pore-structure dependent kinetic adsorption model	6
3 Underlying data basis for H₂O.....	8
3.1 Sample properties	8
3.2 H ₂ O adsorption kinetic and equilibrium data	9
4 Development of a new adsorption kinetic model for H₂O.....	12
4.1 Modeling of the equilibrium part.....	12
4.2 Modeling the kinetic part.....	13
4.2.1 Overview.....	13
4.2.2 Parameter Dependencies.....	14
General approach to obtain temperature and pressure dependencies	14
The fractional uptake contribution coefficient.....	15
The rate of adsorption parameters	16
5 Results and Discussion.....	19
5.1 Parameterization	19
5.1.1 Results for MH800.....	19
5.1.2 Results for TB.....	23
5.2 Extrapolation behavior	27
6 Conclusion and Outlook	29

Frequently used symbols

Greek Symbols

η	Rate of adsorption coefficient
δ	Fractional contribution coefficient
ξ	Relative pressure coefficient
ν	Temperature-related coefficient
α	Relative pressure-related coefficient of Buttersack's equation
β	Relative pressure-related coefficient of Buttersack's equation
ρ	Density

Abbreviation

2D-NLDFT	Two-Dimensional Non-Local Density Functional Theory
DD	Do & Do Model
Hydro-DEK	Double-Exponential Kinetic Model for Water Vapor
MH800	Micro-crystalline Cellulose Hydrothermal Carbonized Char
OFG	Oxygen Functional Group
PSK	Pore-structure dependent Kinetic Adsorption Model
TA	Thermogravimetric Analysis
TB	Torrefied beech wood
VLE	Vapor-Liquid Equilibrium

Chemical formula symbols

CO ₂	Carbon Dioxide
H ₂ O	Water
O ₂	Oxygen

Subscripts

mm	Meso- to macropores
mi	Micropores
ul	Ultra-micropores
Ref	Reference
base	Baseline
equil	Equilibrium

1 Introduction

The recent years have witnessed growing concerns for the environment. Scientists worldwide have devoted enormous research effort to discover solutions for the existing issues, one of which is the development of energy production processes operating based on combustion under oxyfuel conditions. An important research scope in optimizing such oxyfuel-combustion-processes is the investigation of diffusion of gaseous species like CO_2 and H_2O , since mass transport in the porous structure of solid fuel particles can be a limiting factor for the char conversion rate during gasification (Wedler & Span, 2021). Various conversion models consider the mass transfer in terms of effective diffusion coefficients. According to Phounglamcheik et al. (2022), intraparticle diffusion, or pore diffusion, significantly affects the overall reaction rate. As a result, the analysis of pore diffusion of various gaseous components on biomass chars provides important information for the understanding of combustion efficiency.

One approach to describe the mass transport of relevant gases in a more physically sound manner is the experimental investigation of adsorption kinetics since they provide information of the time-dependent diffusion process. However, there is a lack of mathematical models that describe the adsorption kinetics with the coverage of temperature, pressure, and pore-structure. The most recent development that possesses such capacity is the Pore-Structure dependent Kinetic (PSK) model (Wedler & Span, 2021). The model successfully described the adsorption kinetics of CO_2 on two biomass chars dependent on the chars' pore-structures. The PSK model is able to extrapolate the adsorption behavior to higher temperatures and further studies by Eisenbach et al. (2021) applied this model to the adsorption of O_2 on the same chars and achieved the same success. However, further studies of Eisenbach et al. (2023) discovered special behavior of the adsorption of H_2O on these chars. Therefore, a need for a new model emerges that can describe the adsorption kinetics of water vapor on the respective biomass chars.

This work aims to explore various possibilities for the development of a model that predicts the adsorption kinetics of water vapor. Within this scope, the various dependencies of the adsorption behavior of water vapor on pressure, temperature, and chemical and structural properties of the underlying biomass chars are considered. The advantages and drawbacks of the model, as well as suggestions for further studies, will also be discussed within the extent of the report.

2 Adsorption kinetic modeling in char conversion

This section provides an overview of the options of kinetic adsorption modeling for the improvement of char conversion models. Along with this, the Pore-Structure dependent kinetic adsorption (PSK) model is reviewed and capabilities of the PSK model are pointed out.

2.1 Current consideration of pore diffusion in char conversion modeling

Coal gasification is a complex process, with the char gasification step being crucial, especially when reaction rates are influenced by pore diffusion. Gasification of coal involves complex reactions that are separated into distinct stages, including coal pyrolysis, char gasification, and gas phase reactions. Among these, the char gasification process is identified as the rate-determining step, particularly under conditions where the reaction rate is controlled by pore diffusion (Kajitani et al., 2006). To gain deeper insights into this process, researchers have focused on studying the gasification rate of coal char with carbon dioxide at high temperatures and pressures, resulting in the derivation of gasification rate equations and kinetic parameters. A pivotal aspect of this research involves the development of a comprehensive char conversion code (CCK), which takes into account various factors such as surface oxidation, gasification reactions, film diffusion, pore diffusion, ash encapsulation, and annealing (Holland & Fletcher, 2017). With the development of an oxyfuel combustion system in combination with solid fuel particles originating from biomass, the importance of pore diffusion increases. The pore surface area of such biomass chars is significantly increased and makes an investigation of the internal pore structures of chars and how gasification agents penetrate these structures during the gasification process necessary. To replace the currently applied diffusion description in CCK models, Wedler et al. (2017) and Seibel et al. (2016) introduced an experimentally based approach to model effective diffusion coefficients. They applied common adsorption kinetic models, e.g., the isothermal Fickian diffusion model based on the solution of Fick's second law of diffusion. The problem is that those models are limited regarding the experimental temperature and pressure ranges, which are rather narrow. Therefore, a comprehensive pore-structure dependent kinetic adsorption model has been developed by Wedler and Span (2021) to overcome this lack of modeling.

2.2 A Pore-structure dependent kinetic adsorption model

The PSK model (Wedler & Span, 2021) is a very comprehensive model that describes the adsorption kinetics in a time-resolved manner and pore-structure, pressure, and temperature dependent. Wedler & Span considered the contribution of the individual adsorption capacity of three pore regimes to the absolute adsorbed amount of the sample. The model was already parameterized for the adsorption kinetics of CO₂ (Wedler & Span, 2021) and O₂ (Wedler et al., 2021). These studies considered the same biomass char, TB and MH800, as considered in this study.

The development of the model resulted in the following mathematical function:

$$q(t, p, T) = \rho_{m,CO_2} \left[\begin{aligned} & A_{mm} \cdot c_{mm} \cdot \frac{p \cdot k_{mm} \cdot e^{H_{mm}/(R \cdot T)}}{1 + p \cdot k_{mm} \cdot e^{H_{mm}/(R \cdot T)}} \cdot \left(1 - e^{-\frac{t}{a_{mm} \left(\frac{T}{T_{Ref}} \right)^{-n_{mm}}} } \right) \\ & + A_{mi} \cdot c_{mi} \cdot \frac{p \cdot k_{mi} \cdot e^{H_{mi}/(R \cdot T)}}{1 + p \cdot k_{mi} \cdot e^{H_{mi}/(R \cdot T)}} \cdot \left(1 - e^{-\frac{t}{a_{mi} \left(\frac{T}{T_{Ref}} \right)^{-n_{mi}}} } \right) \\ & + A_{ul} \cdot c_{ul} \cdot \frac{p \cdot k_{ul} \cdot e^{H_{ul}/(R \cdot T)}}{1 + p \cdot k_{ul} \cdot e^{H_{ul}/(R \cdot T)}} \cdot \left(1 - e^{-\frac{t}{a_{ul} \left(\frac{T}{T_{Ref}} \right)^{-n_{ul}}} } \right) \end{aligned} \right] \quad (1)$$

The model suggests that the adsorption of CO₂ and O₂ on the two biomass chars is contributed by the adsorption capacity of three pore regimes, including a meso- to macro, a micro, and an ultramicropore-regime. The adsorption of each of the pore regimes consists of an equilibrium part and a kinetic, time-dependent, part. The equilibrium parts are based on the Langmuir isotherm model, while adding the analyzed surface area of each pore regime A_i and the constant c_i related to the average thickness of the sorption layer of the corresponding pore regime. The kinetic part of the model is constructed with a time constant a_i and a constant n_i representing the temperature dependency of the model. By fitting individual parameter sets for each char and gas the PSK model successfully describes the adsorption kinetics of CO₂ and O₂ on TB and MH800, as well as their dependence on the pore distribution of the samples.

The studies of Wedler & Span (2021) and Wedler et al. (2021) also derived some valuable information of the pore diffusion of the two gases from the model. With the fitted parameter sets, mass transfer properties, such as the mass transfer coefficient and the sorption flow rate, were obtained.

Eisenbach et al. (2023) measured the adsorption kinetics for H₂O on the same biomass chars. They found significantly different adsorption behavior and conclusively a new model approach is needed. In the following section the special adsorption behavior of H₂O vapor is emphasized. The presented data are further used for the development of a new model.

3 Underlying data basis for H₂O

This section presents the underlying data basis, which was measured by Eisenbach et al. (2023) and used for the model development in section 4. Furthermore, the correlation between the adsorption behavior and the chemical and structural properties is shown here and discussed briefly.

3.1 Sample properties

The measurements of the adsorption kinetics and equilibria are based on the same biomass char particles as in the studies of Wedler & Span (2021) and Wedler et al. (2021). The production of the hydrochar MH800 involved hydrothermal carbonization with microcrystalline cellulose and water, resulting in a solid fuel devoid of ash and consisting solely of carbon, oxygen, and hydrogen. A subsequent pyrolysis at 800 °C results in a highly porous char. The TB char is a result of a gasification process with CO₂ at 1000 °C. It is known that the two strongest influential factors on the water vapor adsorption behavior originate from the structural constitution of the underlying materials and the degree of functionalization with oxygen containing surface groups (OFG) (Eisenbach et al., 2023; Liu et al., 2017).

As a private communication by T. Eisenbach, detailed information about the pore surface area and the OFG quantity of the individual chars is given. The surface area of the pores at three different pore regimes (meso- to macropores, micropores, and ultra-micropores) as defined by IUPAC (Thommes et al., 2015) is presented in Table 1. According to Thommes et al., pores with width smaller than 0.7 nm are called ultramicropores, while pores with widths from 0.7 to 2 nm are called micropores, and those with widths exceeding 2 nm are grouped as meso- and macro- pores.

Table 1. Pore surface areas obtained from 2D-NLDFT analysis for the TB and MH800 chars.

Surface Area (m ² / g)	TB	MH800
Meso- to Macropores (A_{me})	2.6757	48.4306
Micropores (A_{mi})	45.5725	212.8691
Ultra-micropores (A_{ul})	533.4914	619.9652

Table 2. Oxygen functional group quantities for the TB and MH800 chars.

Oxygen Functional Groups	TB	MH800
C(=O)OH	0.28	0.19
Overall	2.06	1.55

As shown in Table 1, the area of the meso- to macropores and the micropores of MH800 is significantly larger than those of TB. In general, both chars are highly microporous.

Another property that is potentially affecting the adsorption of water vapor on the samples is the oxygen functional group quantity on the surface of the particles. Detailed information of the measurement procedure of OFG is given by Eisenbach et al. (2023). As shown in Table 2, MH800 contains an overall amount of 1.55 mmol/g oxygen functional groups, while TB char possesses a slightly higher concentration of 2.06 mmol/g oxygen functional groups. According to Liu et al. (2017), carboxylic acids are the functional groups that most considerably influence the adsorption of biomass chars, and these carboxylic acid groups also have a slightly higher concentration in TB than in MH800. However, it is still probable that these functional groups can be a factor that induces the special behavior of the adsorption kinetics, as will later be shown. The reason for this expectation is that, as reported by Boehm (1994), due to their hydrophilic characteristics, oxygen functional groups impact considerably on the adsorption process of water vapor. In the following the underlying data basis is presented and discussed briefly as their characteristics are an important factor for the further model development in section 4.

3.2 H₂O adsorption kinetic and equilibrium data

The data basis consists of adsorption kinetics and adsorption equilibria along isotherms. The adsorption data were recorded in a modified gravimetric sorption analyzer ISOSORP by TA instruments, which was equipped with a VLE cell providing the water vapor for the adsorption measurements. The data for MH800 and TB were measured by Eisenbach et al. (2023). The apparatus set up used in the measurement procedures is described in detail by Eisenbach et al. (2023). Both equilibrium values and kinetics of adsorption were measured and recorded at 3 temperatures (approximately 298 K, 308 K, and 318 K) and various relative pressure values ranging from approximately 0.1 to 0.9. The recorded adsorption kinetics appeared to

be stable at 298 K and 308 K, while some measured at 318 K were unreliable. As a result, further analysis in following sections uses kinetics at 298 K and 308 K for the study of model and parameters, while those measured at 318 K are used for the verification of the later developed model.

Exemplarily, Figure 1 displays the equilibrium values for MH800 along the isotherm at 298.65 K and 308.55 K. The isotherm shows low adsorption equilibria at low relative pressure. The maximum uptake increases drastically at middle-range relative pressure, then flattens as the relative pressure continues to approach one. According to Rahman et al. (2019), the isotherm of MH800 is of type V, which indicates that this sample is highly porous and comparatively hydrophobic.

The adsorption kinetics are shown with respect to their individual equilibrium values, representing the fractional uptake. Figure 2 shows the fractional uptakes at several relative pressures and corresponding adsorption temperatures of 298.65 K for MH800. As can be seen, the time required for the kinetics to reach equilibrium varies heavily with relative pressure. There is a tendency of the speed of the kinetics to decrease with increasing relative pressure up to a specific relative pressure, then accelerate again with rising relative pressure. Such behavior is also reported by Fletcher et al. (2007), where the reasoning was suggested to be attributed to the interaction of H₂O with the oxygen functional groups and the pore structure of the sample. This behavior emerges as need to develop an adsorption model that is capable of describing the pressure dependency of the speed of the kinetics.

As shown in Figure 2, a significantly different behavior is displayed by the adsorption of water vapor compared to those of supercritical gases like CO₂ and O₂. As reported by Wedler et al. (2021), the kinetics of CO₂ and O₂ become slower with increasing relative pressure at the same temperature. However, for the case of H₂O, the kinetics become slower to a certain pressure, then faster again close to saturation. Therefore, there is a need for a kinetic adsorption model, which should complement PSK approach for modeling mass transport properties for the special case of H₂O.

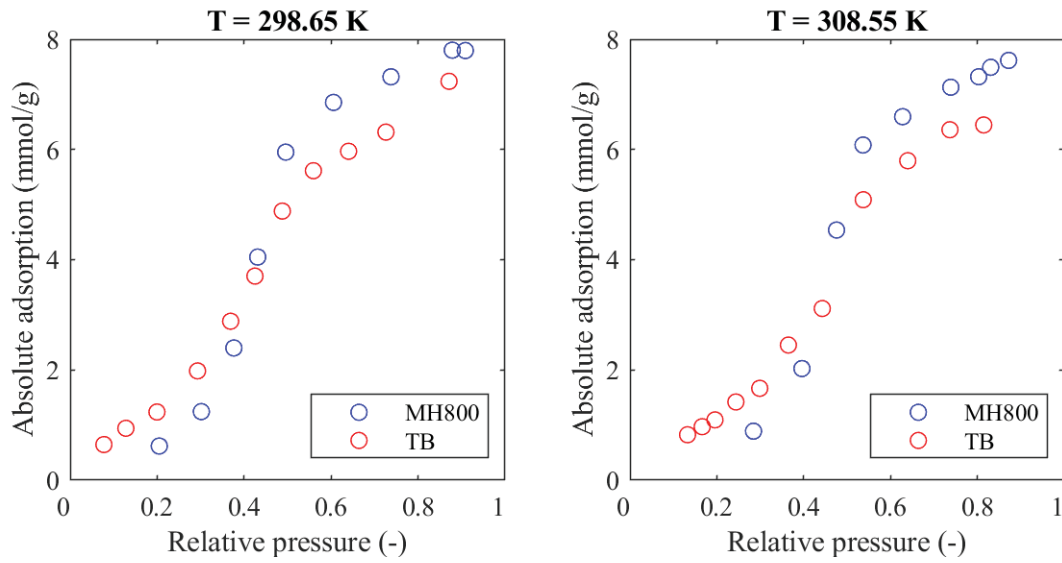


Figure 1. Adsorption isotherms of water vapor on MH800 and TB for two exemplary temperatures.

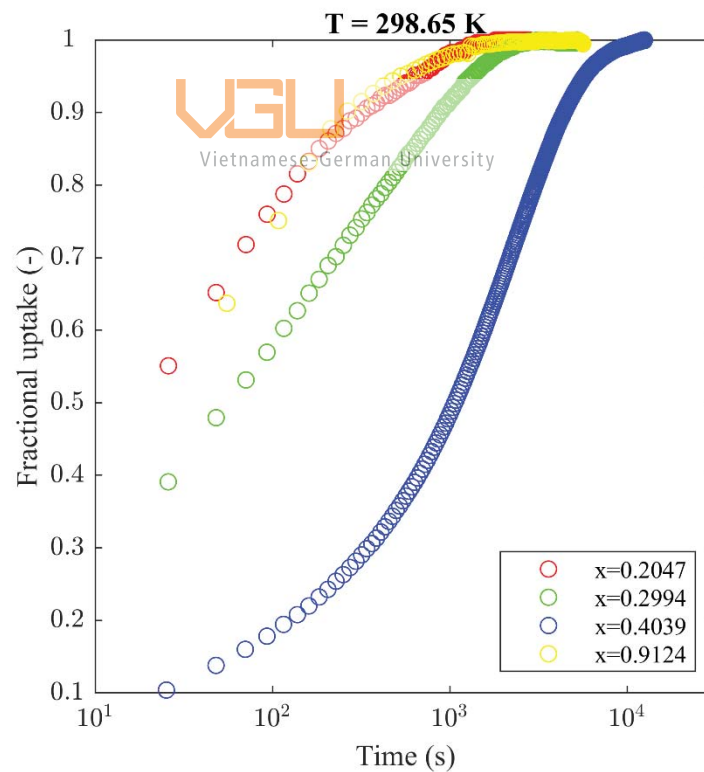


Figure 2. Fractional uptake of kinetics of MH800 at various relative pressures.

4 Development of a new adsorption kinetic model for H₂O

The adsorption model for H₂O vapor attempts to separate the kinetics from the equilibrium part, as it is already realized in the PSK model by Wedler and Span (2021). The equilibrium state is reached when the amount of adsorbed and desorbed gas is equal at any instance. Thus, the kinetic part can be defined as the time-dependent fractional uptake, representing the temporal proportion of uptake of the kinetics. Both parts were developed independently, later combined by the following equation:

$$q(t, p, T) = q_{\text{equil}}(p, T) \cdot \theta(t, p, T) \quad (2)$$

Where $q(t, p, T)$ is the absolute uptake of the kinetics, $q_{\text{equil}}(p, T)$ is the equilibrium loading, and $\theta(t, p, T)$ is the fractional uptake of the kinetics. All terms of the equation are pressure- and temperature-dependent, serving the purpose of predicting the adsorption kinetics of water vapor at any pressure and temperature. In the following two sections the approach for the equilibrium and the kinetic part of the novel adsorption kinetic model for water vapor is presented. In further courses and discussion, the model is named the Hydro Double-Exponential Kinetic (Hydro – DEK) model.

Vietnamese-German University

4.1 Modeling of the equilibrium part

Figure 1 shows the water vapor adsorption isotherms at 298.65 K. According to Rahman et al. (2019), these isotherms are of type V, which is suitable to be presented using the adsorption isotherm model developed by Do & Do (2000). An application of DD model, provided by Buttersack (2019), is applied in this work. The equation of the adsorption isotherm becomes:

$$q_{\text{equil}}(p) = g \cdot \left(f \frac{K_f x \{1 - (1 + \beta)x^\beta + \beta x^{\beta+1}\}}{(1-x)\{1 + (K_f - 1)x - K_f x^{\beta+1}\}} + (1-f) \frac{K_\mu x^\alpha}{1 + K_\mu x^\alpha} \right) \quad (3)$$

Furthermore, the DD model is suitable for the special behavior of H₂O vapor adsorption as it was developed only for adsorption systems considering H₂O. Accordingly, it contains a physical meaning in each parameter.

The parameter x is the relative pressure corresponding to the respective vapor phase pressure and the saturated vapor pressure calculated from the adsorption temperature, K_f is the interaction constant between the water molecules and the oxygen functional groups, K_μ is the

interaction constant between the water molecules and the pores, f is the fractional distribution of the two terms of the equation, α and β are the water cluster sizes, and q_{\max} is the maximum adsorption capacity of the sample. The model suggests that the absolute adsorption of water vapor consists of the adsorption on functional groups and the adsorption on pore surfaces of the sample. The six parameters K_f , K_μ , f , q_{\max} , α , and β are fitted with the measured data, resulting in a model that is capable of representing the equilibrium values of adsorption at an arbitrary relative pressure. However, the model is a classical isotherm model which is only able to represent the pressure dependency of the adsorption equilibria. To establish a temperature dependency to the equilibrium part the six mentioned parameters were fitted with each isotherm, resulting in a set of values corresponding to different temperature of each parameter. Fitting the temperature-dependent data sets of the parameters to Equation (4) provides the temperature dependency of the parameters, where g_i is the parameter that will be described using this function of temperature dependency. The level of dependency on temperature $\nu_{2,i}$ of some parameters may be negative.

$$g_i = \nu_{1,i} \left(\frac{T}{273.15} \right)^{\nu_{2,i}} \quad (4)$$


This temperature dependency equation will also be used in the following sections for the establishment of temperature dependency for parameters of the kinetic part as well.

4.2 Modeling the kinetic part

4.2.1 Overview

As previously described in section 3.2, the fractional uptake of the adsorption kinetics of water vapor is markedly dissimilar to those of CO₂, which has been reported by Wedler & Span (2021) and O₂ by Wedler et al. (2021). As suggest in a study of Fletcher et al. (2007), the adsorption kinetics of samples containing functional groups on the surface area could be fractionized into a proportion with low activation energy (a faster adsorption process), and a proportion with high activation energy (slower adsorption process). As proposed by Fletcher et al. (2007), this work is following the same approach for the kinetic part using the double-exponential model:

$$F = \frac{M_t}{M_\infty} = A_1(1 - e^{-k_1 t}) + (1 - A_1)(1 - e^{-k_2 t}) \quad (5)$$

Where F is the fractional uptake of the overall adsorption kinetic. The fractional uptake is divided into contributions, A_1 being the fraction of the kinetics contribution with low energy of activation, and $1 - A_1$ being the fraction of the kinetic contribution with high energy of activation. Fletcher et al. (2007) suggested that the slow fractional contribution corresponds to high activation energy, while the fast contribution corresponds to low activation energy. Both exponential parts contain the rate of adsorption coefficients k_1 and k_2 . The double-exponential model by Fletcher et al. is considered for the Hydro – DEK model. Here, only the rate of adsorption coefficients is slightly modified to be time constants η_1 and η_2 of the kinetic adsorption process:

$$\theta(t) = \delta \left(1 - e^{-\frac{t}{\eta_1}} \right) + (1 - \delta) \left(1 - e^{-\frac{t}{\eta_2}} \right) \quad (6)$$

Here δ has equal meaning as A_1 of the double-exponential model, while η_1 and η_2 are in the reversed position comparing to k_1 and k_2 respectively. As a result, the adsorption rate coefficients appear in the form of the inversion of parameters k_1 and k_2 .

4.2.2 Parameter Dependencies

The Hydro – DEK model, in contrast to common adsorption kinetic models and the one proposed by Fletcher for water vapor adsorption, should be able to model and predict adsorption kinetics temperature- and pressure- dependent. Usually, adsorption kinetic models are only applied to one experimental adsorption kinetic at a fixed pressure and temperature.

General approach to obtain temperature and pressure dependencies

To develop a pressure dependency of the kinetic part, the fractional uptake function was first fitted for each of the adsorption kinetics, which served as the data basis and as presented in section 2. The values of the three parameters, as well as their corresponding temperature and pressure at which the adsorption process happened, were then collected, and later plotted against relative pressure for each of the temperatures of adsorption. By plotting the parameters in the described manner, the pressure dependency of each of the parameters could be analyzed for each temperature of adsorption. The temperature dependency would then be

studied by comparing the pressure dependency of those parameters along different isotherms.

Due to the fact that kinetic data from two temperatures 298 K and 308 K were reliable, while several kinetics data measured at 318 K appeared to be rather unstable, the temperature dependency of the parameters was determined using the values fitted for kinetics at 298 K and 308 K and Equation (4). The developed model was later tested against the kinetics at 318 K, and the result approved the usage of Equation (4) as the temperature equation for the parameters of the kinetic part.

The fractional uptake contribution coefficient

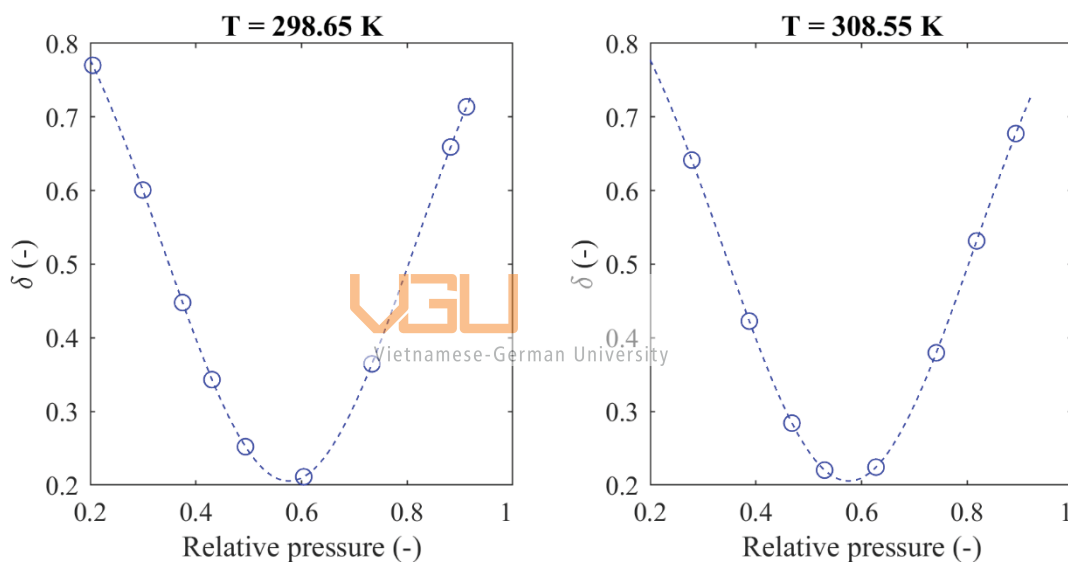


Figure 3. Fractional contribution parameter δ at various relative pressures for MH800 (dashed lines are included to guide the eye)

Figure 3 displays the values of the fractional uptake contribution coefficient δ , which are fitted to the individual and corresponding adsorption kinetics at the stated relative pressures. Exemplarily the temperatures 298.65 K and 308.55 K are chosen. As it is shown in Figure 3, the two datasets for δ show a quadratic-like trend over the relative pressure. A quadratic function appears to be very feasible to display the pressure dependency of the parameter δ . However, it is essential that since δ is a parameter determining the fractional contribution of each fractional uptake contribution, it stays in the range of 0 and 1, with relative pressure

varying from 0 to 1. To guarantee such a condition incorporating a quadratic function, a modified bell-shaped function is used:

$$\delta(x) = 1 - \delta_{\text{base}} e^{0.5 \left(\frac{x - \xi_1}{\xi_2} \right)^2} \quad (7)$$

The function in Equation (7) can describe exactly the behavior of the δ dataset, while maintaining the range condition by adjusting the three coefficients δ_{base} , ξ_1 , and ξ_2 . It is worth noting that the coefficient ξ_1 appears as the axis of symmetry of the function, which may be understood as a flipping point in the relative pressure of the adsorption kinetics.

Various testing attempts suggested that mutual values could be applied to ξ_1 and ξ_2 for both temperatures. Unlike ξ_1 and ξ_2 , no mutual value can be used for δ_{base} in both temperatures. As a result, these two parameters were set as constants since they showed no perceptible dependence on temperature. However, since the dataset was too narrow, this assumption could no longer be correct when the data basis is expanded. Thus, this assumption should be noticed and considered in further studies. To represent the temperature dependency of δ_{base} , Equation (4) was again used.



Vietnamese-German University

The rate of adsorption parameters

Figures 4 and 5 show the fitted values of the two rate of adsorption parameters fitted with the individual adsorption kinetics at the respective temperature and relative pressure. Since η_1 and η_2 display the same pressure dependency and have the same thermodynamics meaning, the same pressure-dependent function was applied. At first glance, both the parameter sets of η_1 and η_2 show a bell curve trend against relative pressure. The values converge to a specific value with increasing and decreasing relative pressure moving away from the axis of symmetry. A slight skewness can also be observed from Figures 4 and 5. Thus, at early trials, a skewed bell curve function was applied to the two parameter sets of η_1 and η_2 . However, further analysis and testing confirmed that this skewness was caused by varying temperature occurring in the measurement (see section 5). Ultimately, a symmetric bell curve function was utilized to describe the pressure dependency of the rate of adsorption parameters. The function is described as follows:

$$\eta_1(x) = a_{\eta_1} e^{-0,5 \left(\frac{x-b_{\eta_1}}{c_{\eta_1}} \right)^2} + \eta_{1,base} \quad (8)$$

$$\eta_2(x) = a_{\eta_2} e^{-0,5 \left(\frac{x-b_{\eta_2}}{c_{\eta_2}} \right)^2} + \eta_{2,base} \quad (9)$$

This pressure dependency is very much similar to the one representing the parameter δ , but reversed in direction. It can be observed from Figures 4 and 5 that the bell curves are all elevated to a certain level, instead of converging to zero like a normal bell curve. This behavior is represented by the coefficients $\eta_{1,base}$ and $\eta_{2,base}$ of the Equations (8) and (9), which may be interpreted as the baseline rate of adsorption at a specific temperature. Coefficients b_{η_i} and c_{η_i} , where i corresponds to the coefficient they belong to, appear as the axis of symmetry and the spread of the curve, respectively. The temperature dependency for the four parameters $a_{\eta_i}, b_{\eta_i}, c_{\eta_i}, \eta_{i,base}$ were later applied using the Equation (4). Coefficients $\nu_{1,i}$ and $\nu_{2,i}$ of each of the four parameters were fitted using the values of the four parameters $a_{\eta_i}, b_{\eta_i}, c_{\eta_i}, \eta_{i,base}$ fitted for the kinetics at 298.65 K and 308.55 K. Once again, the kinetic data measured at 318 K was used as a validation for the values of the model.

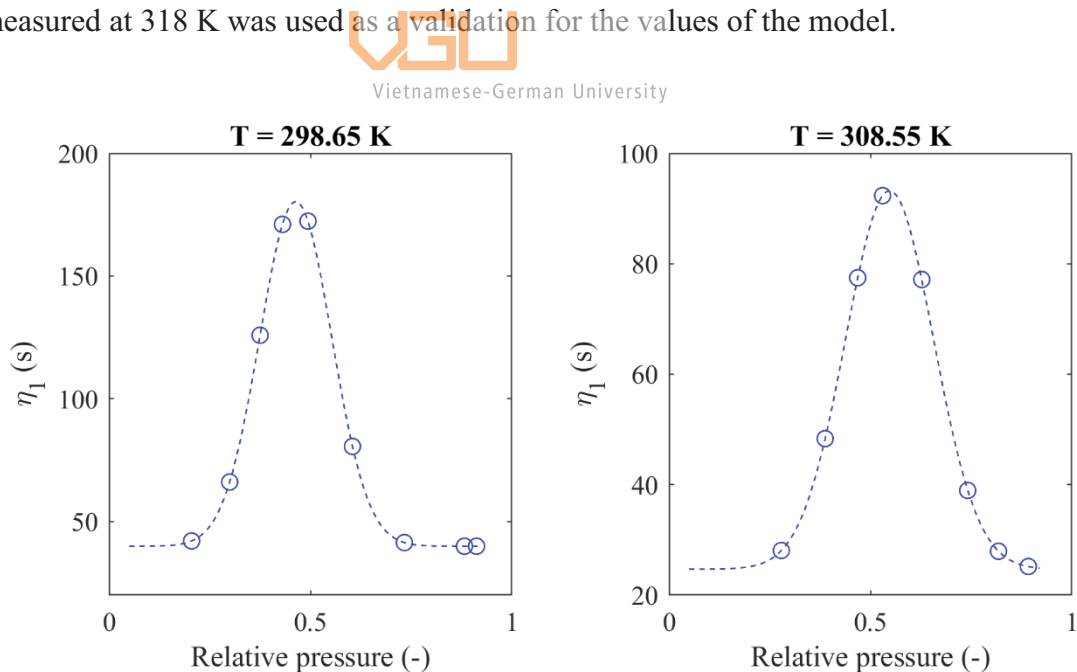


Figure 4. First rate of adsorption parameter η_1 at various relative pressures of MH800 (dashed lines are included to guide the eye)

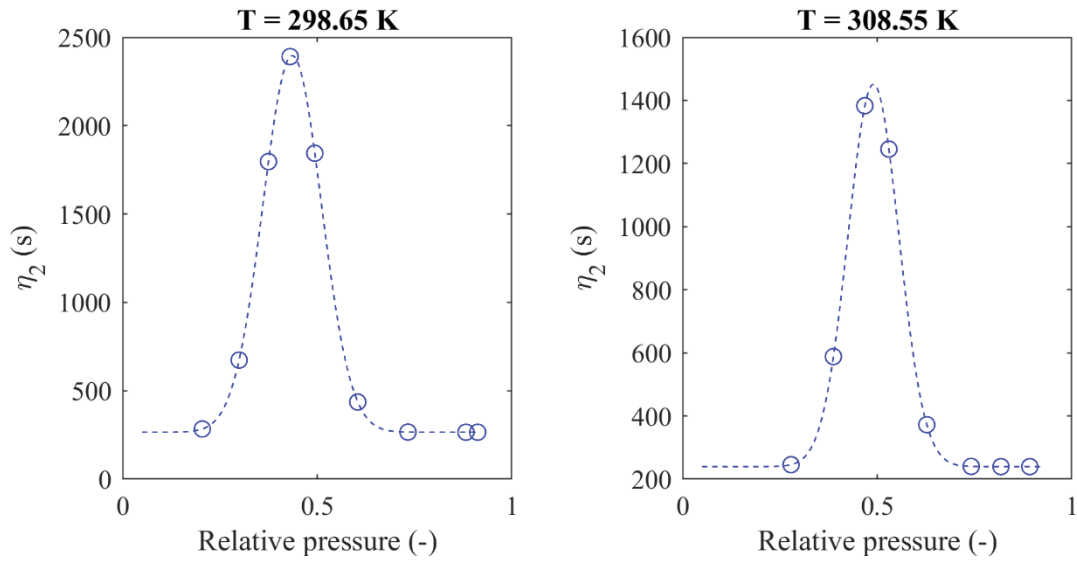


Figure 5. Second rate of adsorption parameter η_2 at various relative pressures of MH800 (dashed lines are included to guide the eye)

It can be inferred from Equation (6) that the larger the value of either of the rate parameters is, the slower the corresponding kinetic contribution takes to reach its own maximum adsorption capacity. It is shown in Figures 4 and 5 that the value range of η_1 is significantly lower than that of η_2 in both temperatures, making η_1 the fast rate coefficient and η_2 the slow rate coefficient. Therefore, parameter δ becomes the fractional contribution of the fast kinetic contribution. It can also be observed that the magnitude of both coefficients decreases with increasing temperature, suggesting that the overall speed of adsorption increases with temperature. Figure 3 indicates that at very low relative pressures (close to 0) or very high relative pressures (close to 1), the contribution of the slow kinetic contribution becomes insignificant.

5 Results and Discussion

5.1 Parameterization

The development of the Hydro – DEK model results in a model that describes the adsorption kinetics of water vapor dependent on pressure and temperature, as described in Equation (10).

$$q(T, p, t) = g \cdot \left(\begin{array}{l} f \frac{K_f x (1 - (1+b)x^b + bx^{b+1})}{(1-x)(1 + (K_f - 1)x - K_f x^{b+1})} \\ + (1-f) \frac{K_\mu x^a}{1 + K_\mu x^a} \end{array} \right) \left(\begin{array}{l} \left(1 - \delta_{\text{base}} e^{-\frac{1}{2} \left(\frac{x - \xi_1}{\xi_2} \right)^2} \right) \left(1 - e^{a_{\eta 1}} e^{-\frac{-t}{\frac{1}{2} \left(\frac{x - b_{\eta 1}}{c_{\eta 1}} \right)^2 + \eta_{1, \text{base}}}} \right) \\ + \delta_{\text{base}} e^{-\frac{1}{2} \left(\frac{x - \xi_1}{\xi_2} \right)^2} \left(1 - e^{a_{\eta 2}} e^{-\frac{-t}{\frac{1}{2} \left(\frac{x - b_{\eta 2}}{c_{\eta 2}} \right)^2 + \eta_{2, \text{base}}}} \right) \end{array} \right) \quad (10)$$



Vietnamese-German University

Where all parameters, except from ξ_1 and ξ_2 , are described by the temperature Equation (4), where $\nu_{1,i}$, $\nu_{2,i}$ represent temperature sensitivity for each temperature-dependent parameter. The values for $\nu_{1,i}$, $\nu_{2,i}$, ξ_1 , and ξ_2 are fitted individually for the two chars – MH800 and TB, and are listed in sections 5.1.1 and 5.1.2 for each of the sample, respectively. The fitting process was done with data measured at 298 K and 308 K.

5.1.1 Results for MH800

Table 3 lists the coefficients of the temperature dependency equation, $\nu_{1,i}$ and $\nu_{2,i}$, applied for every parameter i of the Hydro – DEK model. The negative values of $\nu_{2,i}$ indicate the decrement of the corresponding parameter with increasing temperature. Some of the $\nu_{2,i}$ values appear to be abnormally high for a level of temperature dependency; however, further fitting effort with better constraints can be conducted to refine those values. For

MH800, the values for ξ_1 and ξ_2 are 0.5758 and 0.2356, respectively. These two parameters were set as constants since they showed no perceptible dependence on temperature. However, since the dataset was too narrow, this assumption could no longer be correct.

Table 3. Parameter set of all temperature-dependent parameters of the Hydro—DEK model for MH800

	$V_{1,i}$	$V_{2,i}$
K_f	5.345	-17.88
K_μ	699.9	31.58
a	6.747	5.456
b	2.708	-2.084
f	0.1854	7.598
g	5.574	3.489
δ_{base}	1.062	-3.265
a_{η_1}	1000	-22
b_{η_1}	0.2938	5.106
c_{η_1}	0.05131	6.228
$\eta_{1.\text{base}}$	148.6	-14.73
a_{η_2}	10000	-17.32
b_{η_2}	0.3155	3.619
c_{η_2}	0.1101	-4.302
$\eta_{2.\text{base}}$	350	-3.115
ξ_1		0.5758
ξ_2		0.2356

Figure 6, 7, and 8 show predictions of both fractional and absolute uptake of several measured kinetics for MH800. It can be evaluated that while the fractional uptake curves are predicted rather precisely, several absolute uptake curve predictions show considerable difference. As shown in Figure 9, although the isotherm model provided by Buttersack is able to represent the shape of the isotherm of the equilibria, precision is missing in some data

points. As a result, there may exist a gap between some prediction curves provided by the Hydro – DEK model and the measured data. An example is the absolute adsorption kinetic displayed in Figure 8, which was measured at 322.46 K, relative pressure of 0.6829. It can be observed that, while the fractional uptake was predicted precisely, the prediction for the absolute uptake was not very well predicted due to a misprediction of equilibrium value.

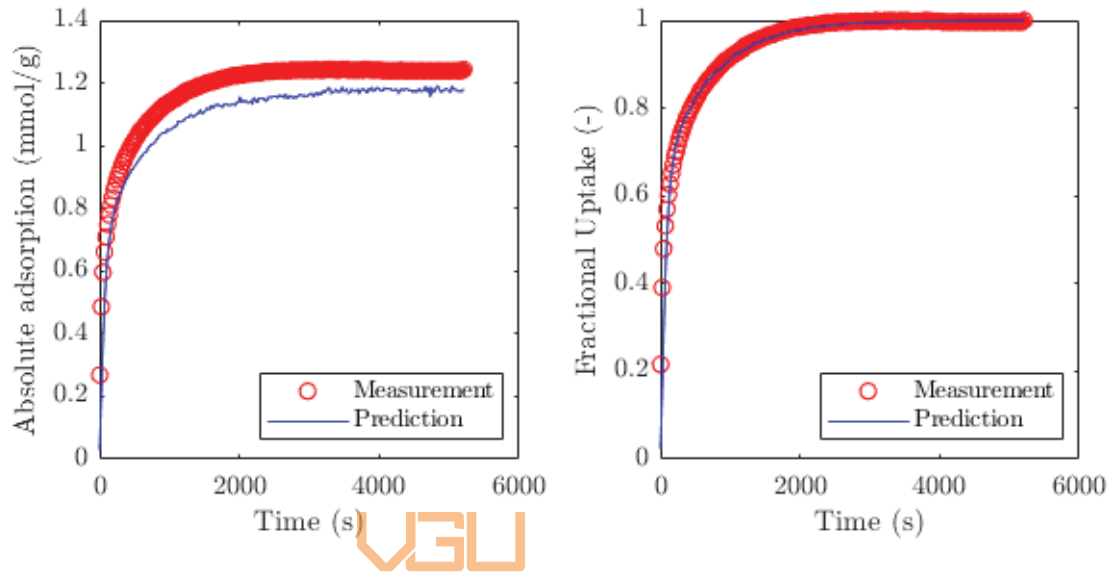


Figure 6. Absolute and fractional uptake of water vapor on MH800 at 298.65 K, relative pressure of 0.2994

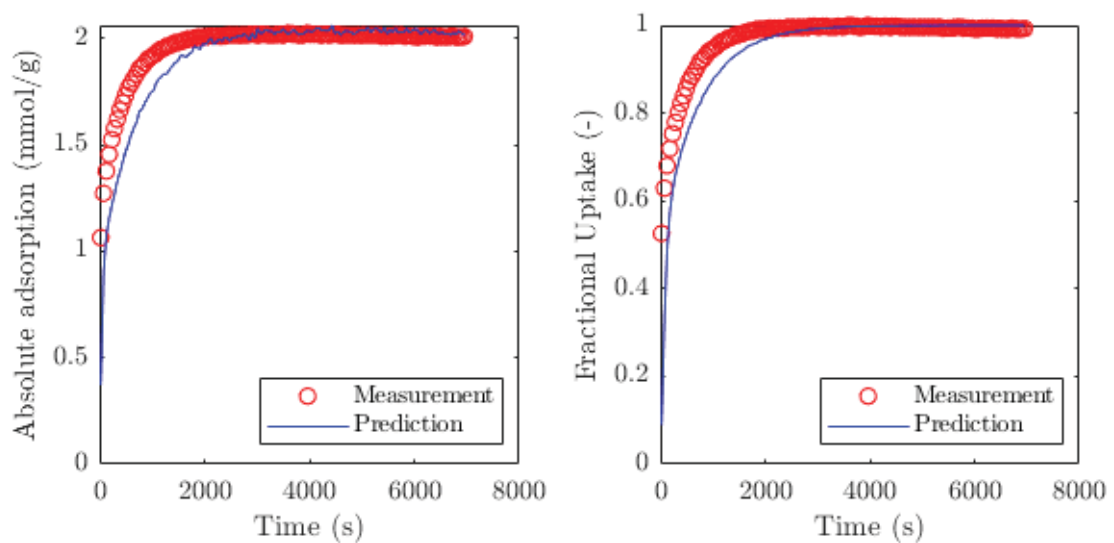


Figure 7. Absolute and fractional uptake of water vapor on MH800 at 308.55 K, relative pressure of 0.3875

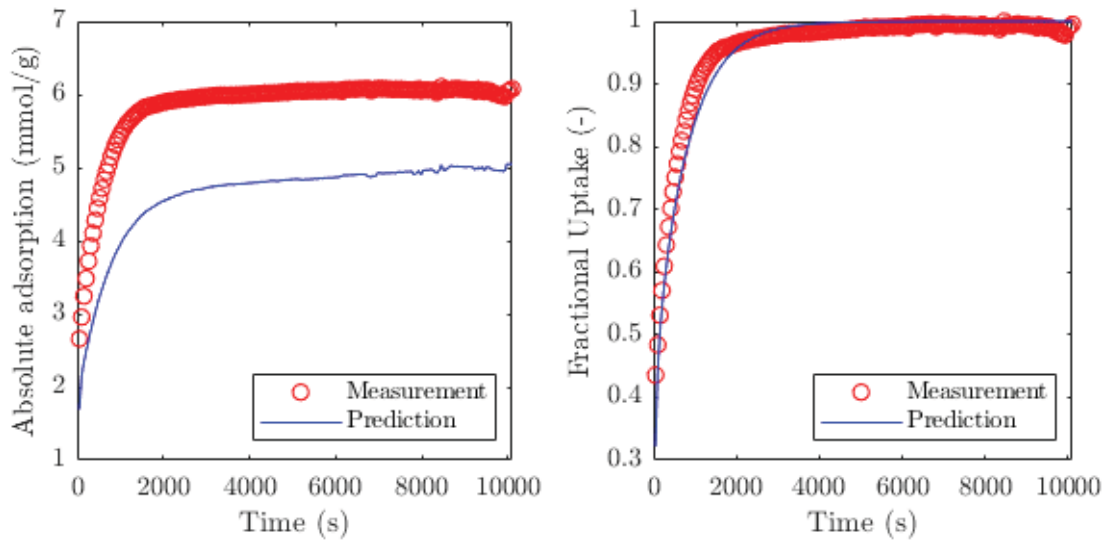


Figure 8. Absolute and fractional uptake of water vapor on MH80 at 322.46 K, relative pressure of 0.6829

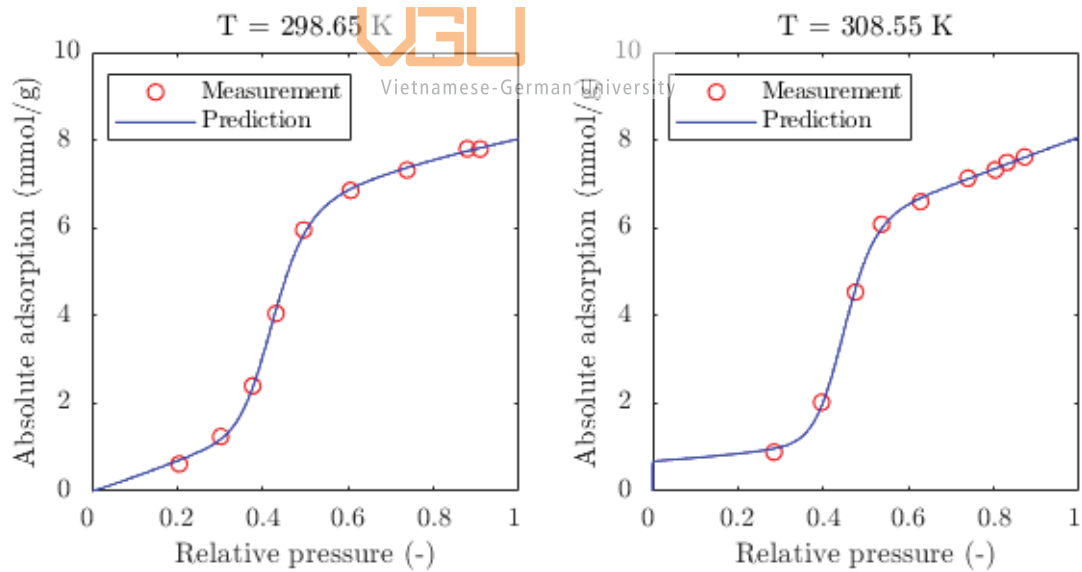


Figure 9. Isotherm fittings of water vapor on MH80

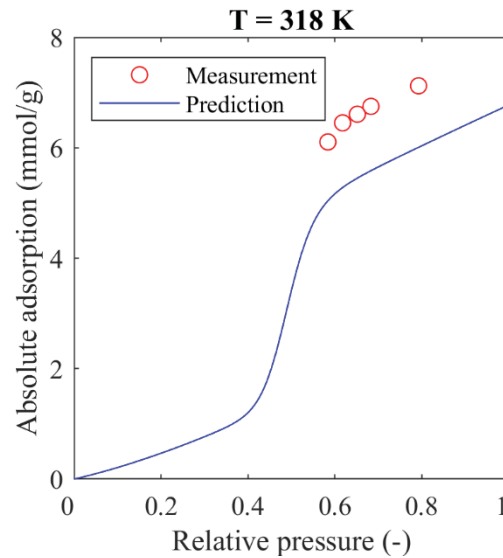


Figure 10. Isotherm prediction of water vapor on MH800 at 318 K

As shown in Figure 10, the prediction curve is very much different from the measured values. Thus, further temperature dependency analysis should be done, including the enrichment of the dataset.



Vietnamese-German University

5.1.2 Results for TB

Values shown in table 4 are the fitted values for the parameters of the Hydro – DEK model applied for TB char. For TB, the values for ξ_1 and ξ_2 are 0.6385 and 0.3324, respectively. As discussed in section 5.1.1, these two parameters were set as constants since they showed no perceptible dependence on temperature. However, since the dataset was too narrow, this assumption could no longer be correct. The same fitting process applied for MH800 was used for the fitting of parameters for TB. It can be observed from the table that the range of values for parameters of the kinetic part stay in the same range as those of MH800. However, the values of parameters in the equilibrium part of the equation appear to be very much different from those fitted for MH800. This behavior implies that further fitting with better constraints should be done to acquire more thermodynamically reasonable sets of parameters. It can be noticed that the value of the parameter v_{2,K_μ} is extremely high, which is certainly unable of representing a physical meaning. As mentioned previously, the establishment of the temperature dependency for the parameters was done based only on the data measured at 298 K and 318 K; thus, the enhancement of the data basis is very much necessary

Table 4. Parameter set of all temperature-dependent parameters of the Hydro—DEK model for TB

	$V_{1,i}$	$V_{2,i}$
K_f	83.26	-33.44
K_μ	5.424	76.82
a	2.97	13.43
b	19.69	-16.93
f	0.2141	8.997
g	1.99	8.967
δ_{base}	0.7747	-0.5098
a_{η_1}	13.35	-9.784
b_{η_1}	0.4532	-0.6327
c_{η_1}	0.02172	2.455
$\eta_{1,\text{base}}$	94.58	-17.42
a_{η_2}	739	-1.099
b_{η_2}	0.3135	3.985
c_{η_2}	0.1326	-1.171
$\eta_{2,\text{base}}$	966.9	-8.322
ξ_1		0.6385
ξ_2		0.3324

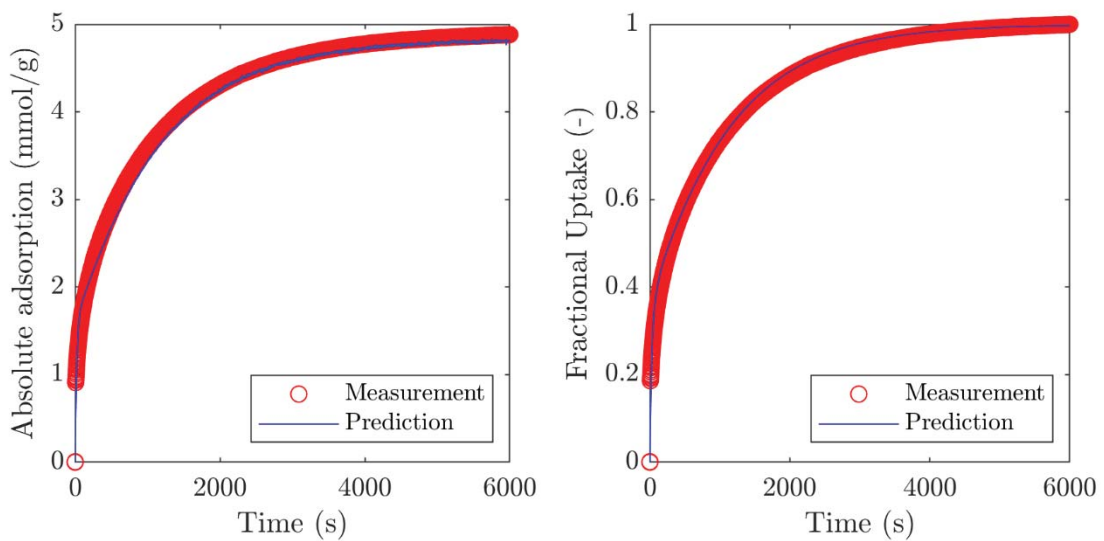


Figure 11. Absolute and fractional uptake of water vapor on TB at 299.12 K, relative pressure of 0.4728

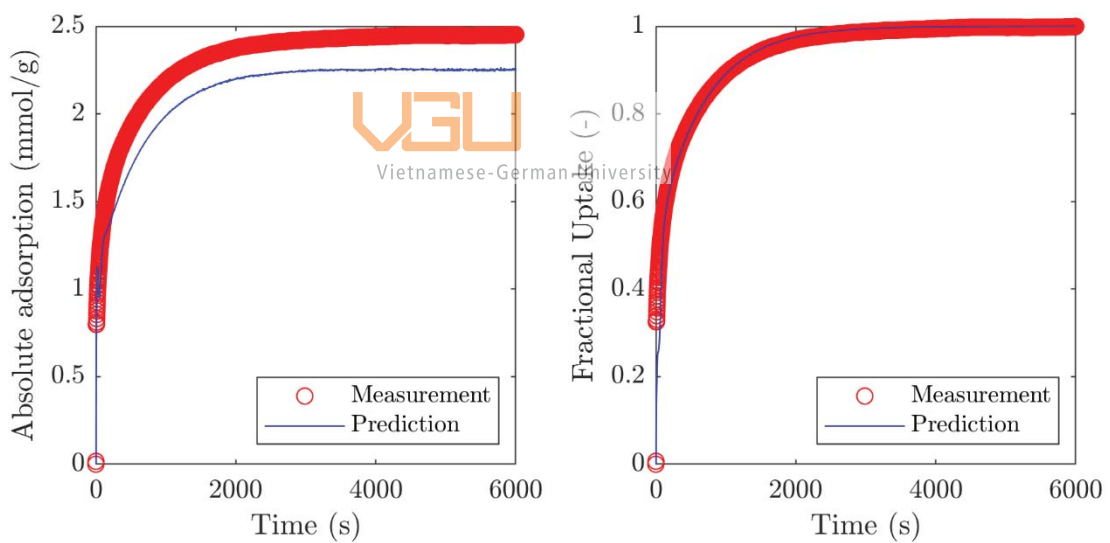


Figure 12. Absolute and fractional uptake of water vapor on TB at 308.29 K, relative pressure of 0.3613

Figures 11, 12, and 13 show the predictions of both fractional and absolute uptake of several measured kinetics for TB. Resembling what is reported in section 5.1.1, the model can well predict the fractional uptake of TB. However, a difference between the prediction and measured data can occur at the absolute adsorption curve, since there exists some difference between the measured data and the predicted isotherm of TB char. As can be seen from Figure 15, the prediction for equilibrium values at 318 K is very much different from measured data, which was caused by the exclusion of this data set from the fitting process.

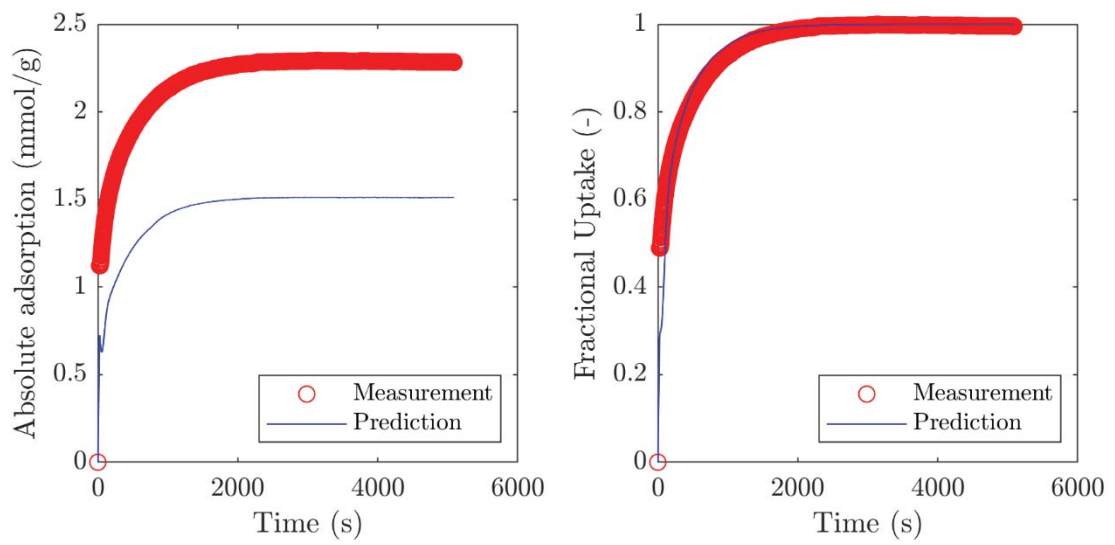


Figure 13. Absolute and fractional uptake of water vapor on TB char at 317.81 K, relative pressure of 0.3850

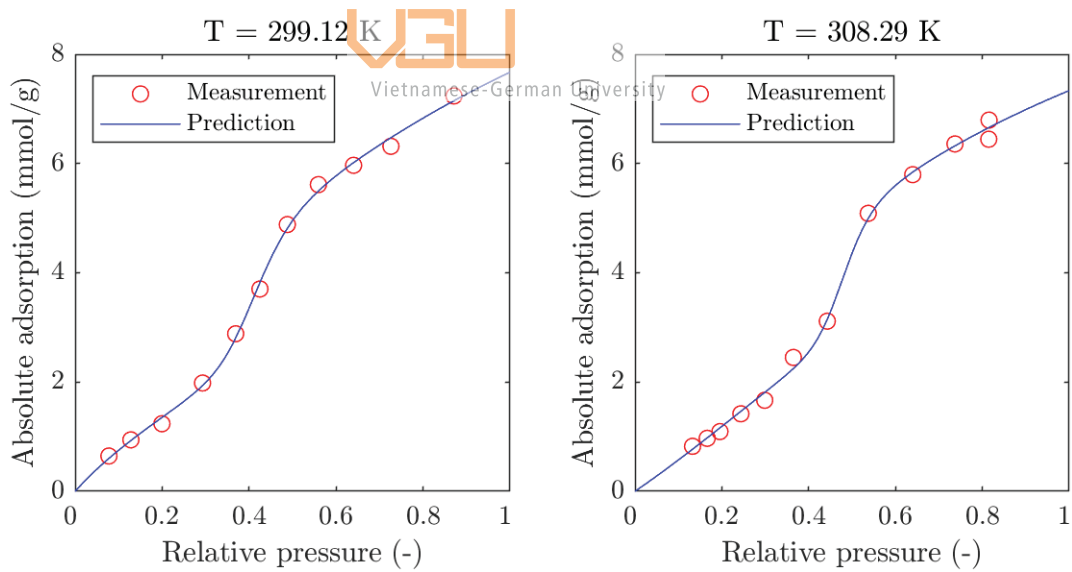


Figure 14. Isotherm fittings of water vapor on TB

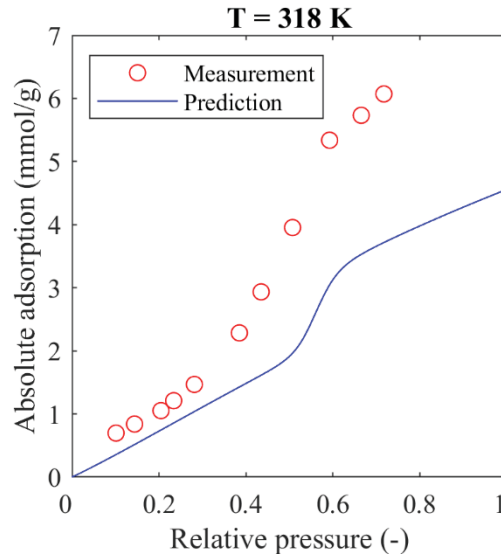


Figure 15. Isotherm prediction of water vapor on MH800 at 318 K

5.2 Extrapolation behavior

The model can also extrapolate to higher temperatures intending to model adsorption kinetics closer to combustion temperatures. The result of the extrapolation of the model to higher temperature looks optimistic, to a certain extent. At high temperature, the kinetics become very fast, which corresponds to what has been expected. However, a significant limit of the model is, it is incapable of extrapolating to temperatures above the super-critical temperature of water vapor, which is 647.1 K (Wagner & Pruß, 2002). The reason is that the pressure dependency of the model is established based on relative pressures. At temperatures above super-critical temperature of water vapor, the saturated vapor pressures are absent, resulting in the indetermination of the equation. Thus, further research should be conducted to find possible solutions to eliminate this limitation so that the model better serves the purpose of predicting water vapor adsorption at combustion temperature.

Several modifications for the Hydro – DEK model can be considered in further studies to correct the existing lack of precision. Firstly, instead of using Equation (2) as the governing equation, one can consider redistributing the kinetics in the following manner:

$$q = q_f \left(1 - e^{-\frac{t}{\tau_f}} \right) + q_\mu \left(1 - e^{-\frac{t}{\tau_\mu}} \right) \quad (11)$$

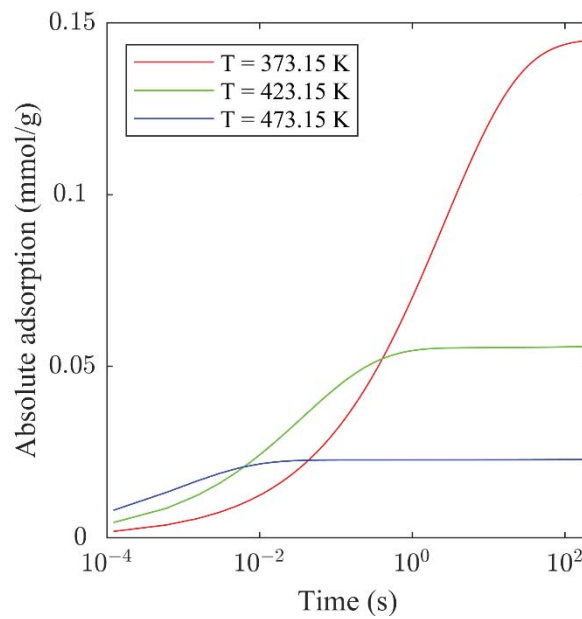


Figure 16. Predictions of kinetic of adsorption at higher temperatures, relative pressure of 0.2

Where η_1 and η_2 maintain their meaning as in previous sections, while q_f and q_μ are maximum adsorption capacity of the functional groups and pores, respectively. With this configuration, the adsorption capacity of the functional groups and the pores to the adsorption kinetics is now directly assigned to their time-dependent component. Thus, the need of parameter δ is eliminated, and the fitting of the parameters of the equilibrium part is more constrained, since such process would be done simultaneously with the fitting of the parameters of the kinetic part. Another possible direction is to modify or reconstruct the isotherm model of Buttersack. Although being able to reproduce the shape of the type V isotherm, the model may not be specific enough for the adsorption of biomass chars. Sample property information such as pore distribution or functional groups concentration can be included to better describe the feature of the biomass chars.

Another issue of the study is the lack of data sets at different temperatures. The temperature dependency of the parameters was analyzed based on the data set of 3 temperatures of 298K, 308K, and 318K. Therefore, a misinterpretation of temperature dependency may happen due to a lack of variety of temperature.

6 Conclusion and Outlook

In general, the double – exponential water vapor adsorption model predicts fairly precisely the adsorption kinetics compared with the measured data. Despite noticeable differences in the maximum uptake occurring at several kinetics, the model successfully reproduced the shape of the kinetics, as well as the special behavior of the adsorption of water vapor. Furthermore, with the ability to cover both temperature and pressure, the model appears to be comprehensive, thus useful to provide an overview of the kinetics of water vapor adsorption at temperatures that measurements are very hard to conduct, i.e., combustion temperatures or lower temperatures.


Beside the advantages shown above, the model displays obvious disadvantages that are very prone to further improvements. With some twenty coefficients, the model appears to be very bulky, causing difficulties in handling and usage. Further improvements can attempt to reduce the number of coefficients by analyzing trends and behaviors of the coefficients with more measured data. What is more, the model is limitedly attached to MH800. Since no sample-based properties are included in the model, the set of coefficients must be fitted again for new samples. This reduces the convenience and comprehensiveness of the model, which were two of the initial purposes of the development of the model. Further research can aim at including such information, such as pore structure or functional group's distribution on the sample's surface area so that the model is capable of predicting various samples. Another issue of the model is that the coefficients do not necessarily bring about a specific thermodynamic meaning, or the meaning is very hard to be derived from the equation itself. Further insights can consider regrouping and combining some of the coefficients together to introduce a specific meaning for it, as well as simplify the current equation. In this work, the data measured at 318 K of both samples were not included in the fitting process, but rather used as a verification for the model. As a result, the equilibrium values at 318 K were not predicted precisely. This is another noticeable drawback of the results of this work. As mentioned above, the temperature dependency of the Hydro–DEK model was established with the data measured at only two temperature values. The kinetic data measured at 318 K was not included in the fitting process, leading to insufficient temperature information. With such an issue, the temperature dependency was not well established, leading to incorrect equilibria predictions. Accordingly, predictions at higher temperature may be unreliable, especially for equilibrium values. Thus, further studies could consider carrying out more kinetic measurements at various temperatures, repeating the same procedure, and analyzing the relationship

of each of the parameters with temperature. Equilibrium data measured at 318 K should also be included in the fitting process to enhance the precision of the equilibrium prediction.

To conclude, the Hydro-DEK model, to a certain extent, successfully represents the adsorption kinetics of water vapor on MH800. As a primitive insight to the special behavior of the adsorption of water vapor on activated carbon, it has favorably delivered such trait into the equation. However, many noticeable limitations are also displayed, which may later become interesting topics for further studies.

References

- Boehm, H. P. (1994). SOME ASPECTS OF THE SURFACE CHEMISTRY OF CARBON BLACKS AND OTHER CARBONS. In *Carbon* (Vol. 32, Issue 5).
- Buttersack, C. (2019). Modeling of type IV and v sigmoidal adsorption isotherms. *Physical Chemistry Chemical Physics*, 21(10), 5614–5626. <https://doi.org/10.1039/c8cp07751g>
- Do, D. D., & Do, H. D. (2000). A model for water adsorption in activated carbon. In *Carbon* (Vol. 38).
- Eisenbach, T., Wedler, C., & Span, R. (2023). *Correlation of chemical and structural pore properties and H2O vapor adsorption in biomass char particles*. <https://www.researchgate.net/publication/370340987>
- Fletcher, A. J., Uygur, Y., & Mark Thomas, K. (2007). Role of surface functional groups in the adsorption kinetics of water vapor on microporous activated carbons. *Journal of Physical Chemistry C*, 111(23), 8349–8359. <https://doi.org/10.1021/jp070815v>
- Holland, T., & Fletcher, T. H. (2017). Comprehensive Model of Single Particle Pulverized Coal Combustion Extended to Oxy-Coal Conditions. *Energy and Fuels*, 31(3), 2722–2739. <https://doi.org/10.1021/acs.energyfuels.6b03387>
- Kajitani, S., Suzuki, N., Ashizawa, M., & Hara, S. (2006). CO₂ gasification rate analysis of coal char in entrained flow coal gasifier. *Fuel*, 85(2), 163–169. <https://doi.org/10.1016/j.fuel.2005.07.024>
- Liu, L., Tan, S. (Johnathan), Horikawa, T., Do, D. D., Nicholson, D., & Liu, J. (2017). Water adsorption on carbon - A review. In *Advances in Colloid and Interface Science* (Vol. 250, pp. 64–78). Elsevier B.V. <https://doi.org/10.1016/j.cis.2017.10.002>
- Phounglamcheik, A., Bäckebo, M., Robinson, R., & Umeki, K. (2022). The significance of intraparticle and interparticle diffusion during CO₂ gasification of biomass char in a packed bed. *Fuel*, 310. <https://doi.org/10.1016/j.fuel.2021.122302>
- Rahman, M. M., Muttakin, M., Pal, A., Shafiullah, A. Z., & Saha, B. B. (2019). A statistical approach to determine optimal models for IUPAC-classified adsorption isotherms. *Energies*, 12(23). <https://doi.org/10.3390/en12234565>
- Seibel, C., Wedler, C., Vorobiev, N., Schiemann, M., Scherer, V., Span, R., & Fieback, T. M. (2016). Sorption measurements for determining surface effects and structure of solid fuels. *Fuel Processing Technology*, 153, 81–86. <https://doi.org/10.1016/j.fuproc.2016.08.004>

-
- Thommes, M., Kaneko, K., Neimark, A. V., Olivier, J. P., Rodriguez-Reinoso, F., Rouquerol, J., & Sing, K. S. W. (2015). Physisorption of gases, with special reference to the evaluation of surface area and pore size distribution (IUPAC Technical Report). *Pure and Applied Chemistry*, 87(9–10), 1051–1069. <https://doi.org/10.1515/pac-2014-1117>
- Wagner, W., & Pruß, A. (2002). The IAPWS formulation 1995 for the thermodynamic properties of ordinary water substance for general and scientific use. *Journal of Physical and Chemical Reference Data*, 31(2), 387–535. <https://doi.org/10.1063/1.1461829>
- Wedler, C., Eisenbach, T., Schwarz, J., & Span, R. (2021). *A first parameterization of the pore-structure dependent kinetic adsorption model for O₂ adsorption in biomass conversion modeling.*
- Wedler, C., Seibel, C., Richter, M., Fieback, T. M., & Span, R. (2017). Oxyfuel Combustion - Experimental Investigation of Sorption Effects on Coal Char. *Energy Procedia*, 105, 1847–1851. <https://doi.org/10.1016/j.egypro.2017.03.540>
- Wedler, C., & Span, R. (2021). A pore-structure dependent kinetic adsorption model for consideration in char conversion – Adsorption kinetics of CO₂ on biomass chars. *Chemical Engineering Science*, 231. <https://doi.org/10.1016/j.ces.2020.116281>
- 
- Vietaamese-German University